Dynamics in the centre manifold of the collinear points of the Restricted Three Body Problem

Àngel Jorba(1) and Josep Masdemont(2)

April 21st, 1997

(1) Departament de Matemàtica Aplicada i Anàlisi, Universitat de Barcelona, Gran Via 585, 08007 Barcelona, Spain. E-mail: angel@maia.ub.es

(2) Departament de Matemàtica Aplicada I, Universitat Politècnica de Catalunya, Diagonal 647, 08028 Barcelona, Spain. E-mail: josep@barquins.upc.es

Abstract

This paper focuses on the dynamics near the collinear equilibrium points $L_{1,2,3}$ of the spatial Restricted Three Body Problem. It is well known that the linear behaviour of these three points is of the type center$\times$center$\times$saddle. To obtain an accurate description of the dynamics in an extended neighbourhood of those points, two different (but complementary) strategies are used.

First, the Hamiltonian of the problem is expanded in power series around the equilibrium point. Then, a partial normal form scheme is applied in order to uncouple (up to high order) the hyperbolic directions from the elliptic ones. Skipping the remainder we have that the (truncated) Hamiltonian has an invariant manifold tangent to the central directions of the linear part. The restriction of the Hamiltonian to this manifold is the so-called reduction to the centre manifold. The study of the dynamics of this reduced Hamiltonian (now with only 2 degrees of freedom) gives a qualitative description of the phase space near the equilibrium point.

Finally, a Lindstedt-Poincaré procedure is applied to explicitly compute the invariant tori contained in the centre manifold. These tori are obtained as the Fourier series of the corresponding solutions, being the frequencies a power expansion of some parameters (amplitudes). This allows for an accurate quantitative description of these regions. In particular, the well known Halo orbits are obtained.

Keywords: center manifolds, normally hyperbolic manifolds, lower dimensional tori, Lissajous orbits, Halo orbits, algebraic manipulators, Lindstedt-Poincaré method.

Contents

1 Introduction

Let us start with a brief description of the so-called Restricted Three Body Problem (from now on, RTBP). Consider the motion of a infinitessimal particle under the gravitational attraction (Newton's law) of two punctual masses called primaries. The attraction of the infinitessimal particle on the primaries has been neglected (as if it had zero mass) so the primaries are describing Keplerian orbits around their common centre of masses. Then, the study of the motion of the infinitessimal particle is what is known as RTBP. Here we will assume (without further mention) that the primaries are moving on a circular orbit, although the case in which they move on a elliptic trajectory is also very relevant. The RTBP is used as a first model to study several problems of Celestial Mechanics. For instance, to study the motion of an asteroid under the attraction of Jupiter and Sun, or the motion of an artificial satellite in the Earth-Moon system.

To simplify the equations of motion, let us take units of mass, length and time such that the sum of masses of the primaries, the gravitational constant and the period of the motion of the primaries is 1, 1 and 2π respectively. With these units the distance between the primaries is also equal to 1. We denote by μ the mass of the smallest primary (the mass of the biggest one is then $1-\mu$), $\mu \in (0, \frac{1}{2}]$. A usual system of reference (called synodical system) is the following: the origin is taken at the centre of masses of the two primaries, the X axis is given by the line that goes from the smallest to the biggest primary (and with this orientation), the Z axis has the direction given by the angular motion of the primaries (and with the same orientation) and the Y axis is chosen to have a positively oriented system of reference. Hence, in the synodical system the primary of mass μ is always located at $(\mu-1,0,0)$ and the primary of mass $1-\mu$ at $(\mu,0,0)$.

Defining momenta as $P_X = \dot{X} - Y$, $P_Y = \dot{Y} + X$ and $P_Z = \dot{Z}$, the equations of motion can be written in Hamiltonian form. The corresponding Hamiltonian function is (see [23])

$$H = \frac{1}{2}(P_X^2 + P_Y^2 + P_Z^2) + YP_X - XP_Y - \frac{1-\mu}{r_1} - \frac{\mu}{r_2}. \tag{1}$$

It is also well-known that the RTBP in synodical coordinates has five equilibrium points. Two of them can be found as the third vertex of the two equilateral triangles that can be formed using the two primaries as vertices (they are also called triangular points, Lagrangian points or simply $L_{4,5}$). The collinear points lay on the X-axis and are also called $L_{1,2,3}$ or Eulerian points (see Figure 1).

In this paper we are going to focus on the dynamics near the collinear points. The linearized vectorfield at these points exhibits a behaviour of the kind centre×centre×saddle (for all μ), so these equilibrium points are unstable. On the other hand, there exist solutions that are always close to them, such as the two families of periodic Lyapunov orbits related to the two linear oscillators of the linearized vectorfield. As one of these families is contained in the horizontal plane and the other one is tangent to the (Z, P_Z) direction at $L_{1,2,3}$, we will refer to them as the planar and vertical (Lyapunov) families, respectively. Other interesting solutions are the two dimensional invariant tori related to the Lissajous solutions, obtained as the product of the two linear oscillations (see [2] and [16] for proofs of the existence of such tori), and the Halo orbits, obtained as a bifurcation of the planar family of Lyapunov orbits.

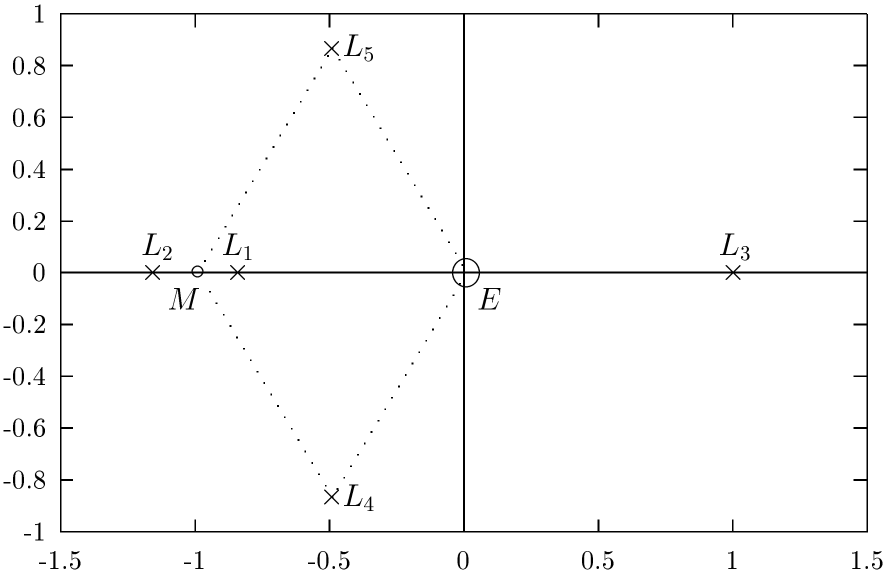

Figure 1: The five equilibrium points of the RTBP.

In order to describe the dynamics in a relatively big neighbourhood of the collinear points, we will perform the so-called reduction to the centre manifold. This process is based on expanding the initial Hamiltonian around a given equilibrium point and performing a partial normal form scheme, uncoupling (up to a high order) the hyperbolic directions from the elliptic ones. The restriction to the invariant manifold tangent to these elliptic directions is a two degrees of freedom Hamiltonian system with an elliptic equilibrium point at the origin. The study of the dynamics of this Hamiltonian is done by fixing an energy level (the phase space is now 3-D) and doing a suitable (2-D) Poincaré section, that can be easily plotted. In this way, varying the value of the energy, we will obtain a sequence of 2-D plots describing the dynamics contained in the centre directions.

Once the dynamics has been qualitatively explained, we face the problem of computing accurately some of the solutions of the centre manifold. To this end we discuss the Lindstedt-Poincaré procedure (see [19]), that is directly applied to the initial equations (the ones related to (1)). This process is based on finding a parametric family of trigonometric expansions that satisfy the equations of motion, up to a sufficiently high order. Once these expansions have been found, it is very easy to plot periodic and quasiperiodic solutions contained in the centre manifold.

The advantage of the Lindstedt-Poincaré method is that the expressions are written in the initial coordinates, and that we have a compact expression for all the trajectories. On the other hand, the reduction to the centre manifold provides an easy way of producing qualitative plots of the dynamics close to the point.

Since 1978, when NASA launched the ISEE-3 spacecraft, Lissajous and Halo type trajectories around the collinear equilibrium points have been considered in the trajectory design of astrodynamic missions. Since the end of 1996 the SOHO spacecraft is using a Halo orbit around L_1 in the Earth-Sun system as a nominal station orbit. Moreover, in a near future more complex missions to the same location are envisioned, such as the GENESIS mission, planned to be launched by the year 2001 (see also [3], [4], [10], [11], [12] and [22]). Semianalytical expansions up to a high order, like the ones obtained by the Lindstedt-Poincaré procedure, can give accurate trajectories for the RTBP model, that can be easily improved for more realistic models for the motion of the spacecraft in the solar system ([6], [9]). The initial approximation is, in many cases, only slightly deformed when it is recomputed for a realistic model (under some extra hipotheses, [17] contains some theoretical results about the effect of the main perturbations of these kind of problems on previously existing periodic and quasiperiodic solutions). Hence, the knowledge of all the librating trajectories given by the reduction to the centre manifold allows to select a very suitable approximation for a given purpose. We note the flexibility of this design process, simplifying the study of complex missions and giving a fast adequation to the technical requirements.

Let us remark that all the computations mentioned here have been done using algebraic manipulators written from scratch (in C and Fortran) by the authors, taking advantage of the particularities of the problem. This, jointly with the use of double precision coefficents for the involved expansions, allows to obtain the results presented here within a reasonable amount of computer time and memory. A general purpose algebraic manipulator is not efficient enough to produce these results using actually existing computers (see also [13]).

Finally, let us mention that the computation of the centre manifold to obtain a complete description of the dynamics was first considered (as far as we know) in [6], in order to describe a big neighbourhood of the L_1 point of the Earth-Sun system. Related computations can be found in [15], [20] and [1]. The Lindstedt-Poincaré method is first described in [19], and it has been used in many contexts (see, for instance, [7] or [6]).

The paper has been organized as follows: In Section 2 we introduce the equations of motion as well as the expansions used; Section 3 is devoted to the reduction to the centre manifold and Section 4 contains the details of the computation of invariant tori near the collinear equilibrium points. A discussion of the results is also contained in sections 3 and 4.

2 Expansion of the equations of motion

The equations of motion corresponding to (1) are usually written as

$$\begin{aligned} \ddot{x} - 2\dot{y} &= \frac{\partial \Omega}{\partial x}, \\ \ddot{y} + 2\dot{x} &= \frac{\partial \Omega}{\partial y}, \\ \ddot{z} &= \frac{\partial \Omega}{\partial z}, \end{aligned} \tag{2}$$

where $\Omega = \frac{1}{2}(x^2 + y^2) + (1 - \mu)/r_1 + \mu/r_2$. Let us start by translating the origin of coordinates to the selected point $L_{1,2,3}$. It is well known ([23]) that the distance from

L_j to the closest primary, γ_j, is given by the only positive solution of the Euler quintic equation,

$$\gamma_j^5 \mp (3-\mu)\gamma_j^4 + (3-2\mu)\gamma_j^3 - \mu\gamma_j^2 \pm 2\mu\gamma_j - \mu = 0, \quad j=1,2,$$
$$\gamma_j^5 + (2+\mu)\gamma_j^4 + (1+2\mu)\gamma_j^3 - (1-\mu)\gamma_j^2 - 2(1-\mu)\gamma_j - (1-\mu) = 0, \quad j=3,$$

where the upper sign in the first equation is for L_1 and the lower one for L_2. These equations can be solved numerically by the Newton method, using as starting point $(\mu/3)^{1/3}$ for the first equation ($L_{1,2}$ cases), and $1-\frac{7}{12}\mu$ for the second one (L_3 case).

In order to have good numerical properties for the coefficients of the Taylor expansion it is very convenient to introduce some scaling (see [21]). The translation to the equilibrium point plus the scaling is given by

$$\begin{aligned} X &= \mp\gamma_j x + \mu + a, \\ Y &= \mp\gamma_j y, \\ Z &= \gamma_j z, \end{aligned}$$

where the upper sign corresponds to $L_{1,2}$, the lower one to L_3, $a = -1+\gamma_1$ for L_1, $a = -1-\gamma_2$ for L_2 and $a = \gamma$ for L_3. Note that this change redefines the unit of distance as the distance from the equilibrium point to the closest primary. As scalings are not canonical transformations, they have to be applied on the equations of motion (2). In order to expand the nonlinear terms, we will use that

$$\frac{1}{\sqrt{(x-A)^2+(y-B)^2+(z-C)^2}} = \frac{1}{D}\sum_{n=0}^{\infty}\left(\frac{\rho}{D}\right)^n P_n\left(\frac{Ax+By+Cz}{D\rho}\right),$$

where $D^2 = A^2+B^2+C^2$, $\rho^2 = x^2+y^2+z^2$ and P_n is the polynomial of Legendre of degree n. After some calculations, one obtains that the equations of motion can be written as

$$\begin{aligned} \ddot{x} - 2\dot{y} - (1+2c_2)x &= \frac{\partial}{\partial x}\sum_{n\geq 3} c_n(\mu)\rho^n P_n\left(\frac{x}{\rho}\right), \\ \ddot{y} + 2\dot{x} + (c_2-1)y &= \frac{\partial}{\partial y}\sum_{n\geq 3} c_n(\mu)\rho^n P_n\left(\frac{x}{\rho}\right), \\ \ddot{z} + c_2 z &= \frac{\partial}{\partial z}\sum_{n\geq 3} c_n(\mu)\rho^n P_n\left(\frac{x}{\rho}\right), \end{aligned} \tag{3}$$

where the left-hand side contains the linear terms and the right-hand side contains the nonlinear ones. The coefficients $c_n(\mu)$ are given by

$$\begin{aligned} c_n(\mu) &= \frac{1}{\gamma_j^3}\left((\pm 1)^n\mu + (-1)^n\frac{(1-\mu)\gamma_j^{n+1}}{(1\mp\gamma_j)^{n+1}}\right), \quad \text{for } L_j,\ j=1,2 \\ c_n(\mu) &= \frac{(-1)^n}{\gamma_3^3}\left(1-\mu+\frac{\mu\gamma_3^{n+1}}{(1+\gamma_3)^{n+1}}\right), \quad \text{for } L_3. \end{aligned}$$

As usual, in the first equation, the upper sign is for L_1 and the lower one for L_2. Note that these equations can be written in Hamiltonian form, by defining the momenta $p_x = \dot{x} - y$, $p_y = \dot{y} + x$ and $p_z = \dot{z}$. The corresponding Hamiltonian is then given by

$$H = \frac{1}{2}\left(p_x^2 + p_y^2 + p_z^2\right) + yp_x - xp_y - \sum_{n\geq 2} c_n(\mu)\rho^n P_n\left(\frac{x}{\rho}\right). \tag{4}$$

The nonlinear terms of this Hamiltonian can be expanded by means of the well-known recurrence of the Legendre polynomials P_n. For instance, if we define

$$T_n(x,y,z) = \rho^n P_n\left(\frac{x}{\rho}\right), \tag{5}$$

then, it is not difficult to check that T_n is a homogeneous polynomial of degree n that satisfies the recurrence

$$T_n = \frac{2n-1}{n} xT_{n-1} - \frac{n-1}{n}(x^2+y^2+z^2)T_{n-2}, \tag{6}$$

starting with $T_0 = 1$ and $T_1 = x$.

2.1 Preliminaries for the centre manifold

The linearization around the equilibrium point is given by the second order terms (linear terms must vanish) of the Hamiltonian that, after some rearranging, takes the form,

$$H_2 = \frac{1}{2}\left(p_x^2 + p_y^2\right) + yp_x - xp_y - c_2x^2 + \frac{c_2}{2}y^2 + \frac{1}{2}p_z^2 + \frac{c_2}{2}z^2. \tag{7}$$

It is not difficult to derive intervals for the values of c_2 when $\mu \in [0, \frac{1}{2}]$ (see Figure 2). As $c_2 > 0$ (for the three collinear points), the vertical direction is an harmonic oscillator with frequency $\omega_2 = \sqrt{c_2}$. As the vertical direction is already uncoupled from the planar ones, in what follows we will focus on the planar directions, i.e.,

$$H_2 = \frac{1}{2}\left(p_x^2 + p_y^2\right) + yp_x - xp_y - c_2x^2 + \frac{c_2}{2}y^2, \tag{8}$$

where, for simplicity, we keep the name H_2 for the Hamiltonian.

The next step will be to compute a symplectic change of variable such that Hamiltonian (8) takes a simpler form, suitable to start the normal form computations. To this end, let us define the 4×4 matrix J as

$$J = \begin{pmatrix} 0 & I_2 \\ -I_2 & 0 \end{pmatrix},$$

where I_2 denote the 2×2 identity matrix. The equations of motion of (8) are given by the linear system

$$\begin{pmatrix} \dot{x} \\ \dot{y} \\ \dot{p}_x \\ \dot{p}_y \end{pmatrix} = J\nabla H_2 = J\mathrm{Hess}(H_2)\begin{pmatrix} x \\ y \\ p_x \\ p_y \end{pmatrix}.$$

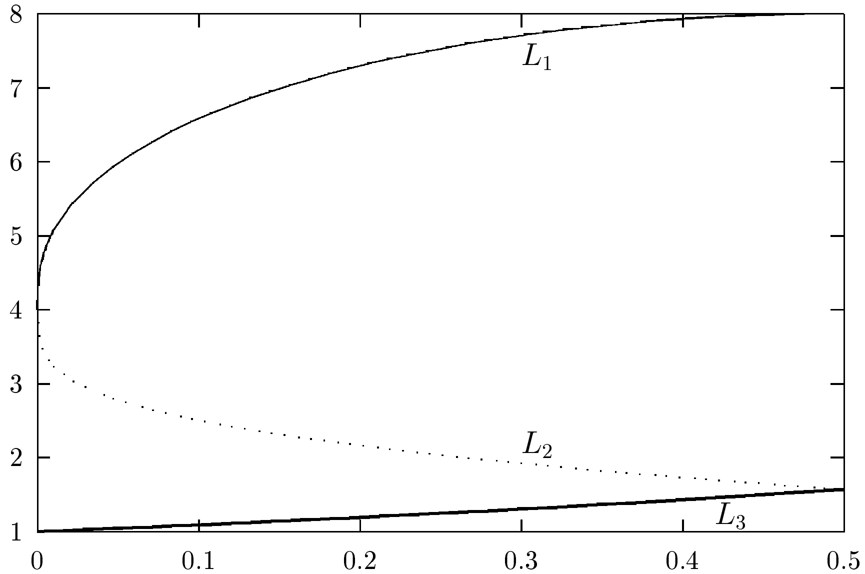

Figure 2: Values of $c_2(\mu)$, $\mu \in [0, \frac{1}{2}]$, for the cases $L_{1,2,3}$.

Let us define the matrix M as $J\mathrm{Hess}(H_2)$,

$$M = \begin{pmatrix} 0 & 1 & 1 & 0 \\ -1 & 0 & 0 & 1 \\ 2c_2 & 0 & 0 & 1 \\ 0 & -c_2 & -1 & 0 \end{pmatrix}. \tag{9}$$

The characteristic polynomial is $p(\lambda) = \lambda^4 + (2 - c_2)\lambda^2 + (1 + c_2 - 2c_2^2)$. Calling $\eta = \lambda^2$, we have that the roots of $p(\lambda) = 0$ are given by

$$\eta_1 = \frac{c_2 - 2 - \sqrt{9c_2^2 - 8c_2}}{2}, \qquad \eta_2 = \frac{c_2 - 2 + \sqrt{9c_2^2 - 8c_2}}{2}.$$

As $\mu > 0$, we have that $c_2 > 1$ that forces $\eta_1 < 0$ and $\eta_2 > 0$. This shows that the equilibrium point is a center$\times$center$\times$saddle. Thus, let us define ω_1 as $\sqrt{-\eta_1}$ and λ_1 as $\sqrt{\eta_2}$. For the moment, we do not specify the sign taken for each square root (this will be discussed later on).

Now, we want to find a symplectic linear change of variables casting (8) into its real normal form and, hence, we will look for the eigenvectors of matrix (9). We will take advantage of the special form of this matrix: if we denote by M_λ the matrix $M - \lambda I_4$, then

$$M_\lambda = \begin{pmatrix} A_\lambda & I_2 \\ B & A_\lambda \end{pmatrix}, \qquad A_\lambda = \begin{pmatrix} -\lambda & 1 \\ -1 & -\lambda \end{pmatrix}, \qquad B = \begin{pmatrix} 2c_2 & 0 \\ 0 & -c_2 \end{pmatrix}.$$

Now, the kernel of M_λ can be found as follows: denoting as $(w_1^\top, w_2^\top)^\top$ the elements of the kernel, we start solving $(B - A_\lambda^2)w_1 = 0$ and then $w_2 = -A_\lambda w_1$. Thus, the eigenvectors of M are given by $(2\lambda, \lambda^2 - 2c_2 - 1, \lambda^2 + 2c_2 + 1, \lambda^3 + (1 - 2c_2)\lambda)^\top$, where λ denotes one of the eigenvalues.

Let us start considering the eigenvectors related to ω_1. From $p(\lambda) = 0$, we obtain that ω_1 verifies

$$\omega_1^4 - (2 - c_2)\omega_1^2 + (1 + c_2 - 2c_2^2) = 0.$$

We also apply $\lambda = \sqrt{-1}\omega_1$ to the expression of the eigenvector and, separating real and imaginary parts as $u_{\omega_1} + \sqrt{-1}v_{\omega_1}$ we obtain

$$\begin{aligned} u_{\omega_1} &= (0, -\omega_1^2 - 2c_2 - 1, -\omega_1^2 + 2c_2 + 1, 0)^\top, \\ v_{\omega_1} &= (2\omega_1, 0, 0, -\omega_1^3 + (1 - 2c_2)\omega_1)^\top. \end{aligned}$$

Now, let us consider the eigenvalues related to $\pm\lambda_1$,

$$\begin{aligned} u_{+\lambda_1} &= (2\lambda_1, \lambda_1^2 - 2c_2 - 1, \lambda_1^2 + 2c_2 + 1, \lambda_1^3 + (1 - 2c_2)\lambda_1)^\top, \\ v_{-\lambda_1} &= (-2\lambda_1, \lambda_1^2 - 2c_2 - 1, \lambda_1^2 + 2c_2 + 1, -\lambda_1^3 - (1 - 2c_2)\lambda_1)^\top. \end{aligned}$$

We consider, initially, the change of variables $C = (u_{+\lambda_1}, u_{\omega_1}, v_{-\lambda_1}, v_{\omega_1})$. To know whether this matrix is symplectic or not, we check $C^\top JC = J$. It is tedious but not difficult to see that

$$C^\top JC = \begin{pmatrix} 0 & D \\ -D & 0 \end{pmatrix}, \qquad D = \begin{pmatrix} d_{\lambda_1} & 0 \\ 0 & d_{\omega_1} \end{pmatrix}.$$

This implies that we need to apply some scaling on the columns of C in order to have a symplectic change. The scaling is given by the square root of the factors

$$d_{\lambda_1} = 2\lambda_1((4 + 3c_2)\lambda_1^2 + 4 + 5c_2 - 6c_2^2), \qquad d_{\omega_1} = \omega_1((4 + 3c_2)\omega_1^2 - 4 - 5c_2 + 6c_2^2).$$

Thus, we define $s_1 = \sqrt{d_{\lambda_1}}$ and $s_2 = \sqrt{d_{\omega_1}}$. As we want the change to be real, we have to ask $d_{\lambda_1} > 0$ and $d_{\omega_1} > 0$. It is not difficult to check that this condition is satisfied for $0 < \mu \le \frac{1}{2}$ in all the points $L_{1,2,3}$, provided that λ_1 and ω_1 have been selected with positive sign.

To obtain the final change, we have to take into account the vertical direction (z, p_z): to put it into real normal form we use the substitution

$$z \to \frac{1}{\sqrt{\omega_2}} z, \qquad p_z \to \sqrt{\omega_2} p_z.$$

This implies that the final change is given by the symplectic matrix

$$C = \begin{pmatrix} \frac{2\lambda_1}{s_1} & 0 & 0 & \frac{-2\lambda_1}{s_1} & \frac{2\omega_1}{s_2} & 0 \\ \frac{\lambda_1^2 - 2c_2 - 1}{s_1} & \frac{-\omega_1^2 - 2c_2 - 1}{s_2} & 0 & \frac{\lambda_1^2 - 2c_2 - 1}{s_1} & 0 & 0 \\ 0 & 0 & \frac{1}{\sqrt{\omega_2}} & 0 & 0 & 0 \\ \frac{\lambda_1^2 + 2c_2 + 1}{s_1} & \frac{-\omega_1^2 + 2c_2 + 1}{s_2} & 0 & \frac{\lambda_1^2 + 2c_2 + 1}{s_1} & 0 & 0 \\ \frac{\lambda_1^3 + (1 - 2c_2)\lambda_1}{s_1} & 0 & 0 & \frac{-\lambda_1^3 - (1 - 2c_2)\lambda_1}{s_1} & \frac{-\omega_1^3 + (1 - 2c_2)\omega_1}{s_2} & 0 \\ 0 & 0 & 0 & 0 & 0 & \sqrt{\omega_2} \end{pmatrix}, \tag{10}$$

that casts Hamiltonian (7) into its real normal form,

$$H_2 = \lambda_1 x p_x + \frac{\omega_1}{2}(y^2 + p_y^2) + \frac{\omega_2}{2}(z^2 + p_z^2). \tag{11}$$

To simplify the computations, we have used a complex normal form for H_2 because this allows to solve very easily the homological equations that determine the generating functions used during the computations of the centre manifold (see Section 3.1). This complexification is given by

$$\begin{array}{rclrclrcl} x &=& q_1, & y &=& \dfrac{q_2 + \sqrt{-1}p_2}{\sqrt{2}}, & z &=& \dfrac{q_3 + \sqrt{-1}p_3}{\sqrt{2}}, \\ p_x &=& p_1, & p_y &=& \dfrac{\sqrt{-1}q_2 + p_2}{\sqrt{2}}, & p_z &=& \dfrac{\sqrt{-1}q_3 + p_3}{\sqrt{2}}, \end{array} \tag{12}$$

and it puts (11) into its complex normal form,

$$H_2 = \lambda_1 q_1 p_1 + \sqrt{-1}\omega_1 q_2 p_2 + \sqrt{-1}\omega_2 q_3 p_3, \tag{13}$$

being λ_1, ω_1 and ω_2 real (and positive) numbers.

2.2 Preliminaries for the Lindstedt-Poincaré

For the computation of the invariant tori we use a Lindstedt-Poincaré method. As this requires to substitute trigonometric expansions into the right-hand side of (3), we will use a recurrent expression for these nonlinear terms. From (5) we define

$$R_{n-1}(x,y,z) = \frac{1}{y}\frac{\partial T_{n+1}}{\partial y}.$$

Obviously, R_{n-1} is a polynomial of degree $n-1$. Moreover we have the identities

$$R_{n-1}(x,y,z) = \frac{1}{z}\frac{\partial T_{n+1}}{\partial z}, \qquad \frac{\partial T_{n+1}}{\partial z} = (n+1)T_n.$$

So, the equations of motion can be written as

$$\begin{aligned} \ddot{x} - 2\dot{y} - (1+2c_2)x &= \sum_{n\geq 2} c_{n+1}(n+1)T_n, \\ \ddot{y} + 2\dot{x} + (c_2 - 1)y &= y\sum_{n\geq 2} c_{n+1}R_{n-1}, \\ \ddot{z} + c_2 z &= z\sum_{n\geq 2} c_{n+1}R_{n-1}. \end{aligned} \tag{14}$$

Note that to substitute an expansion into the right-hand side of (14), one can substitute into the recurrence satisfied by those terms: for the T_n one can use (6) and, for the R_n, it is not difficult to see that

$$R_n(x,y,z) = \frac{2n+3}{n+2}xR_{n-1} - \frac{2n+2}{n+2}T_n - \frac{n+1}{n+2}\rho^2 R_{n-2},$$

where $R_0 = -1$ and $R_1 = -3x$. The expansions that appear in this section have already been used in [7].

3 Reduction to the centre manifold

The process of reduction to the centre manifold is very similar to a normal form calculation. It is based on removing some monomials in the expansion of the Hamiltonian, in order to produce an invariant manifold tangent to the elliptic directions of H_2. Let us recall that, if $F(q,p)$ and $G(q,p)$ are two functions (where, as usual, q denotes the positions and p the momenta), their Poisson bracket is defined as

$$\{F,G\} = \frac{\partial F}{\partial q}\frac{\partial G}{\partial p} - \frac{\partial F}{\partial p}\frac{\partial G}{\partial q}.$$

In what follows, we will use the following notation. If $x = (x_1, \dots, x_n)$ is a vector of complex numbers and $k = (k_1, \dots, k_n)$ is an integer vector, we denote by x^k the value $x_1^{k_1} \cdots x_n^{k_n}$ (in this context we define 0^0 as 1). Moreover, we define $|k|$ as $\sum_j |k_j|$.

3.1 The Lie series method

Let us start by expanding the initial Hamiltonian around the equilibrium point, in the complex coordinates for which the second degree terms are in diagonal form (see Section 2.1). This expansion can be obtained by substituting the linear change given in (10) into the recurrence (6), that is then applied to compute the last sum in (4). The second degree terms in (4) that are not in the summatory are obtained by direct substitution. In this way, the Hamiltonian takes the form

$$H(q,p) = H_2(q,p) + \sum_{n\geq 3} H_n(q,p), \tag{15}$$

where H_2 is given in (13) and H_n denotes an homogeneous polynomial of degree n.

The changes of variables are implemented by means of the Lie series method: if $G(q,p)$ is a Hamiltonian system, then the function $\hat{H}$ defined by

$$\hat{H} \equiv H + \{H,G\} + \frac{1}{2!}\{\{H,G\},G\} + \frac{1}{3!}\{\{\{H,G\},G\},G\} + \cdots, \tag{16}$$

is the result of applying a canonical change to H. This change is the time one flow corresponding to the Hamiltonian G. G is usually called the generating function of the transformation (16). See [5] and references therein for more details.

It is easy to check that, if P and Q are two homogeneous polynomials of degree r and s respectively, then $\{P,Q\}$ is a homogeneous polynomial of degree $r+s-2$. This property is very useful to implement in a computer the transformation (16): for instance, let us assume that we want to eliminate the monomials of degree 3 of (15), as it is usually done in a normal form scheme. Let us select as a generating function a homogeneous polynomial of degree 3, G_3. Then, it is immediate to check that the terms of $\hat{H}$ satisfy

degree 2: $\hat{H}_2 = H_2$,

degree 3: $\hat{H}_3 = H_3 + \{H_2, G_3\}$, degree 4: $\hat{H}_4 = H_4 + \{H_3, G_3\} + \frac{1}{2!}\{\{H_2, G_3\}, G_3\}$,

$\vdots$

Hence, to kill the monomials of degree 3 one has to look for a G_3 such that $\{H_2, G_3\} = -H_3$. Let us denote

$$H_3(q,p) = \sum_{|k_q|+|k_p|=3} h_{k_q,k_p} q^{k_q} p^{k_p}, \quad G_3(q,p) = \sum_{|k_q|+|k_p|=3} g_{k_q,k_p} q^{k_q} p^{k_p},$$

and $H_2(q,p) = \sum_{j=1}^{3} \eta_j q_j p_j$, where $\eta_1 = \lambda_1$, $\eta_2 = \sqrt{-1}\omega_1$ and $\eta_3 = \sqrt{-1}\omega_2$. As

$$\{H_2, G_3\} = \sum_{|k_q|+|k_p|=3} \langle k_p - k_q, \eta \rangle\, g_{k_q,k_p} q^{k_q} p^{k_p}, \quad \eta = (\eta_1, \eta_2, \eta_3),$$

it is immediate to obtain

$$G_3(q,p) = \sum_{|k_q|+|k_p|=3} \frac{-h_{k_q,k_p}}{\langle k_p - k_q, \eta \rangle} q^{k_q} p^{k_p},$$

that is well defined because the condition $|k_q|+|k_p| = 3$ implies that $\langle k_p - k_q, \eta \rangle$ is different from zero. Note that G_3 is so easily obtained because of the "diagonal" form of H_2 given in (13).

In this paper we are not interested in a complete normal form, but only in uncoupling the central directions from the hyperbolic one. Hence, it is not necessary to cancel all the monomials in H_3 but only some of them. There are several ways of doing this uncoupling (see [14]). The one we have used here is based on killing the monomials $q^{k_q}p^{k_p}$ such that the first component of k_q is different from the first component of k_p. This implies that the generating function G_3 is

$$G_3(q,p) = \sum_{(k_q,k_p)\in\mathcal{S}_3} \frac{-h_{k_q,k_p}}{\langle k_p - k_q, \eta \rangle} q^{k_q} p^{k_p}, \tag{17}$$

where $\mathcal{S}_n$, $n \geq 3$, is the set of indices (k_q, k_p) such that $|k_q| + |k_p| = n$ and the first component of k_q is different from the first component of k_p. Then, the transformed Hamiltonian $\hat{H}$ takes the form

$$\hat{H}(q,p) = H_2(q,p) + \hat{H}_3(q,p) + \hat{H}_4(q,p) + \cdots, \tag{18}$$

where $\hat{H}_3(q,p) \equiv \hat{H}_3(q_1p_1, q_2, p_2, q_3, p_3)$ (note that $\hat{H}_3$ depends on the product q_1p_1, not on each variable separately). This process can be carried out up to a finite order N, to obtain a Hamiltonian of the form

$$\bar{H}(q,p) = \bar{H}_N(q,p) + R_N(q,p),$$

where $H_N(q,p) \equiv H_N(q_1p_1, q_2, p_2, q_3, p_3)$ is a polynomial of degree N and R_N is a remainder of order $N+1$ (note that H_N depends on the product q_1p_1 while the remainder depends on the two variables q_1 and p_1 separately). Now, neglecting the remainder and applying the canonical change given by $I_1 = q_1 p_1$, we obtain the Hamiltonian $\bar{H}_N(I_1, q_2, p_2, q_3, p_3)$ that has I_1 as a first integral. Then, setting $I_1 = 0$ (this is to skip the hyperbolic behaviour) we obtain a two degrees of freedom Hamiltonian, $\bar{H}_N(0, \bar{q}, \bar{p})$, $\bar{q} = (q_2, q_3)$, $\bar{p} = (p_2, p_3)$, that represents (up to some finite order N) the dynamics inside the centre manifold. Finally, the Hamiltonian is realified by using the inverse change of (12).

It is interesting to note the absence of small divisors in all the process. The denominators that appear in the generating functions (like (17)), $\langle k_p - k_q, \eta \rangle$, can be bounded from below when $(k_q, k_p) \in \mathcal{S}_N$: using that η_1 is real and that $\eta_{2,3}$ are purely imaginary, we have

$$|\langle k_p - k_q, \eta \rangle| \geq |\lambda_1|, \qquad \text{for all } (k_q, k_p) \in \mathcal{S}_N, \quad N \geq 3.$$

For this reason, the divergence of this process is very mild (for a discussion of this phenomenon, see [14]). This is clearly observed when this process is stopped at some degree N. Then, the remainder is very small in a quite big neighbourhood of the equilibrium point. We will deal with these points in the next section.

An explicit expression for the change of variables that goes from the coordinates of the centre manifold to the coordinates corresponding to Hamiltonian (15) can be obtained in the following way: once the generating function G_3 has been obtained, we can compute

$$\begin{aligned} \tilde{q}_j &= q_j + \{q_j, G_3\} + \frac{1}{2!}\{\{q_j, G_3\}, G_3\} + \frac{1}{3!}\{\{\{q_j, G_3\}, G_3\}, G_3\} + \cdots, && (19) \\ \tilde{p}_j &= p_j + \{p_j, G_3\} + \frac{1}{2!}\{\{p_j, G_3\}, G_3\} + \frac{1}{3!}\{\{\{p_j, G_3\}, G_3\}, G_3\} + \cdots, && (20) \end{aligned}$$

that produces the transformation that sends the coordinates of (15), given by the variables $(\tilde{q}, \tilde{p})$ into the coordinates of (18), represented by the variables (q, p). In the next step, the generating function G_4 is applied to the right-hand side of equations (19) and (20), to obtain the change corresponding to fourth order, and so on. Then, substituting $q_1 = p_1 = 0$ one obtains six power expansions (corresponding to the six initial variables), each one depending on the four variables of the centre manifold. Finally, these expansions are realified in the same way as the Hamiltonian.

3.2 Numerical results

We have implemented the Lie series method to obtain the (approximate) centre manifold for the equilibrium points $L_{1,2,3}$.

3.2.1 Software

As the commercial algebraic manipulators are not efficient enough to deal with big expansions, we have written our own software from scratch, using C language. Here we will only give a brief explanation of the program, but full details of the software (as well as the source code) can be found in [13].

The software consists of several layers. In the bottom layer there are the routines that handle homogeneous polynomials. At this level, an homogeneous polynomial is an array of coefficients (of any kind). To know the exponent of the monomial that corresponds to each coefficient we use the position of the coefficient inside the array. To this end we have written a couple of functions that, given a position inside the array, return the exponent and viceversa. It is very important to code these functions very efficiently, since they have a big impact in the performance of the package. For this paper we have used double precision variables (either real or complex) for the coefficients, since this is enough for our purposes. Of course, it would be possible to use another kind of objects as coefficients, like multiple precision numbers or intervals. For this computation we have taken into account a symmetry of the Hamiltonian: in the power expansion (4), all the monomials such that the sum of the exponents of z and p_z is an odd number are missing. This property is preserved along all the process, and it allows a reduction of the computer time and memory by a factor close to 2.

In the next level we have coded the basic operations with homogeneous polynomials, like products or Poisson brackets, as well as the input/output routines (to read and write homogeneous polynomials). We have also defined a power expansion (of finite order) as an array of homogeneous polynomials. All these things are very easy to implement using the routines of the bottom layer. Finally, in the top level, we have the routines responsible for the algorithm: they expand the Hamiltonian (as it has been explained in Section 2.1) up to some order N and, for each degree, they compute the generating function and transform the Hamiltonian, up to degree N. Finally, the resulting Hamiltonian is restricted to the centre manifold (that is, we substitute $q_1 = p_1 = 0$ in the final Hamiltonian) and realified. Note that the same scheme (with minor modifications) can be used to obtain the corresponding changes of variables.

Finally, let us mention that this software has been run on a Linux PC (using the GNU compiler gcc/g++, version 2.7.2) with a 200 MHz. Pentium Pro CPU. Each centre manifold computation, up to order 32, took about 15h 30' and 38 Megs. of RAM memory. Note that a single expansion like (4) contains 1,388,577 monomials.

3.2.2 The L_1 point of the Earth-Sun system

We have applied the above-explained algorithm to the collinear points of the RTBP. As a first example we have focus on the L_1 point corresponding to the mass parameter $\mu = 3.0404233984441761 \times 10^{-6}$. This is an approximate value for the Earth-Sun case. All the expansions have been performed up to degree $N = 32$.

The first terms of the Hamiltonian restricted to the centre manifold are in Table 1. In order to have an idea of the radius of convergence of this series, we have computed (numerically) the values

$$r_n^{(1)} = \frac{\|H_n\|_1}{\|H_{n-1}\|_1}, \quad r_n^{(2)} = \sqrt[n]{\|H_n\|_1}, \quad \text{where} \quad \|H_n\|_1 = \sum_{|k|=n} |h_k|, \quad 3 \le n \le N, \tag{21}$$

being h_k the coefficient of the monomial of exponent k. These values have been plotted in Figure 4. They seem to show a mild divergence (of logarithmic type, see [14]) of the series, although the size of the region where the (truncated) series looks convergent is quite big. Very realistic estimates of the radius of convergence are obtained as follows: take an

k_1	k_2	k_3	k_4	h_k	k_1	k_2	k_3	k_4	h_k
2	0	0	0	1.0432267821115535e+00	0	0	2	2	1.2424817827573600e-01
0	2	0	0	1.0432267821115544e+00	4	1	0	0	-2.0023568581469642e-01
0	0	2	0	1.0076053314983200e+00	2	3	0	0	3.4353440405951968e-01
0	0	0	2	1.0076053314983200e+00	0	5	0	0	-2.0187593581785741e-02
2	1	0	0	6.5165140304211688e-01	2	1	2	0	-1.9849089558605101e-01
0	3	0	0	-4.1659670417917148e-02	0	3	2	0	1.4712780865620459e-01
0	1	2	0	5.3911539423589860e-01	0	1	4	0	-2.7451664895216100e-02
4	0	0	0	-8.5787309100706366e-02	3	0	1	1	-1.1415906236784655e-01
2	2	0	0	4.1161447802927803e-01	1	2	1	1	2.1573064571205472e-01
0	4	0	0	-2.6563655599297287e-02	1	0	3	1	-9.4058985172178297e-02
2	0	2	0	-1.4043712336878425e-01	2	1	0	2	1.9372724033920288e-01
0	2	2	0	2.7927960671292551e-01	0	3	0	2	-4.4040459096995777e-02
0	0	4	0	-5.7468618566454702e-02	0	1	2	2	1.9106055501181426e-01
1	1	1	1	6.2490402334472867e-02	1	0	1	3	3.8405228183256930e-02
2	0	0	2	1.5018398762952467e-01	0	1	0	4	-2.2759839111536957e-02
0	2	0	2	-2.8803507814853090e-02					

Table 1: Coefficients, up to degree 5, of the Hamiltonian restricted to the centre manifold corresponding to the L_1 point of the Earth-Sun system. The exponents (k_1, k_2, k_3, k_4) refer to the variables (q_2, p_2, q_3, p_3), in this order.

initial condition inside the centre manifold and, by means of a numerical integration of the reduced Hamiltonian, produce a sequence of points for the corresponding trajectory. Then, by means of the change of variables, send these points back to the initial RTBP coordinates. Finally, by means of a numerical integration of the RTBP, we can test if those points belong to the same orbit (note that we can not use a very long time span for those integrations, since the hyperbolic character of the center manifold in the RTBP amplifies the errors exponentially). This gives an idea of the global error we have in the determination of the centre manifold. In fact, the accuracy of the plots in Figures 3 and 6 has been checked in this way.

To have a description of the dynamics inside the centre manifold we use the following scheme: we take the 3D Poincaré section $q_3 = 0$ (this corresponds, at first order, to use $z = 0$ in the sinodical coordinates) and we fix an energy level h_0 to obtain a 2D section. Hence, to obtain a picture of the phase space of this Poincaré section we select a value h_0 and an initial point (q_2, p_2). Using that $q_3 = 0$ and that the value of the Hamiltonian must be h_0, we compute (numerically) the corresponding value p_3 (in fact, there are two values that solve the equation, one positive and one negative; we use the positive one). Then, this point is used as initial condition for a numerical integration of the Hamiltonian restricted to the central part, plotting a point each time that the trajectory crosses the plane $q_3 = 0$ with $p_3 > 0$.

The results can be seen in Figure 3. As the Hamiltonian is positive definite at the origin (this is clearly seen looking at the sign of the coefficients of the second degree terms in Table 1), each energy level defines a closed region in the Poincaré section. The boundary of this region coincides with a periodic orbit of the planar Lyapunov family of

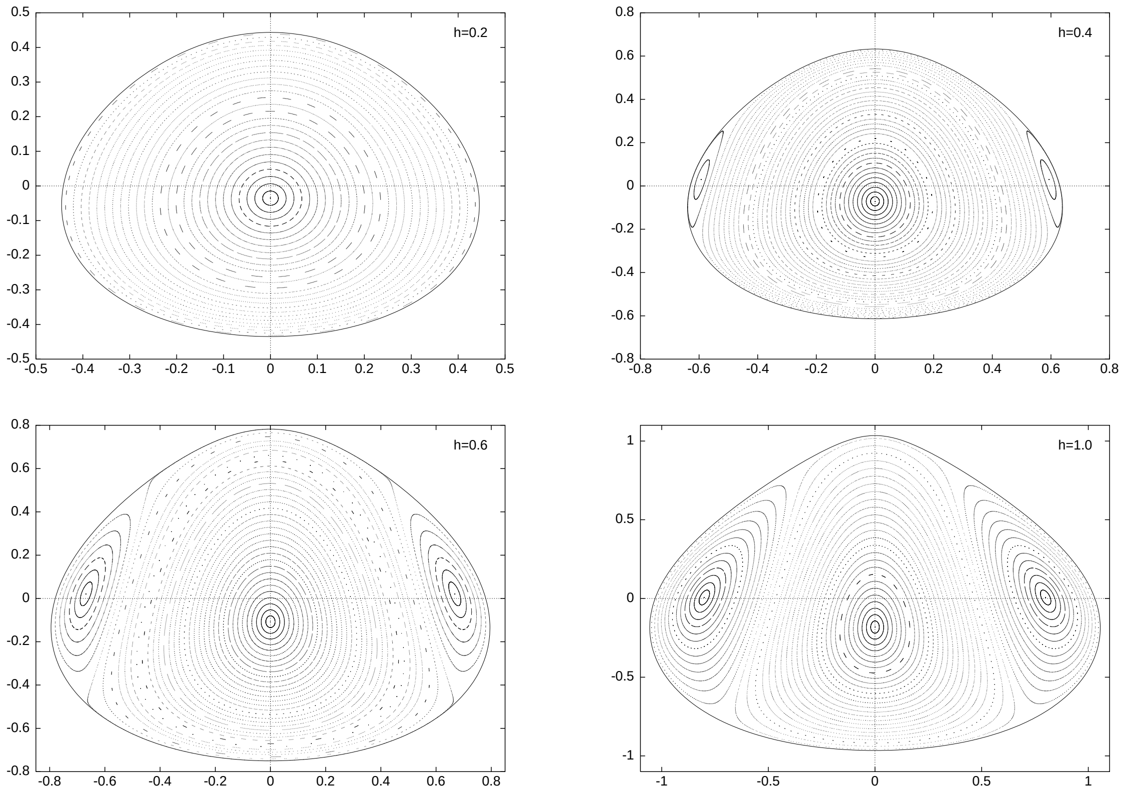

Figure 3: Poincaré sections of the centre manifold of L_1, corresponding to $h = 0.2$, 0.4 0.6 and 1.0.

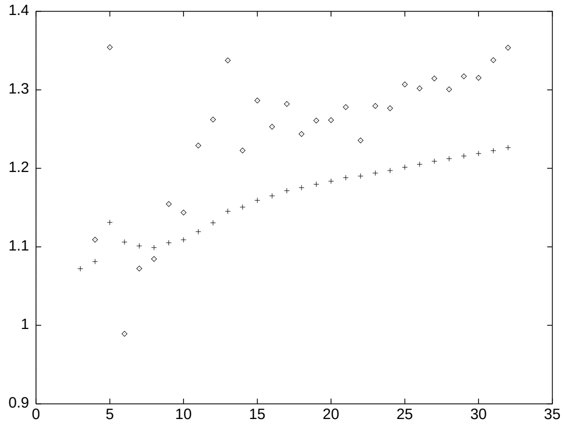

Figure 4: Horizontal axis: values of n. Vertical axis: the corresponding values of $r_n^{(1)}$ ($\diamond$) and $r_n^{(2)}$ ($+$) according to (21), for the L_1 case.

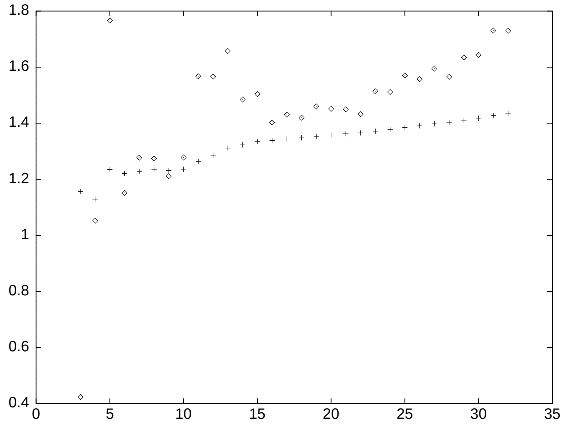

Figure 5: Horizontal axis: values of n. Vertical axis: the corresponding values of $r_n^{(1)}$ ($\diamond$) and $r_n^{(2)}$ ($+$) according to (21), for the L_2 case.

L_1, that is fully contained in the plane $q_3 = p_3 = 0$, and in the figure it has been plot using a continuous line. The motion inside this region is clearly quasiperiodic (except by some gaps that are too small to appear in these pictures), with a fixed point on the p_1 axis, that corresponds to a vertical Lyapunov orbit. If the value of the energy increases, one can see how the well known Halo orbits are born, as a bifurcation of the planar Lyapunov family. Note that the Halo orbits are surrounded by 2D invariant tori (see also [8] and [9]). The boundary between the tori around the Halo orbit and the tori around the vertical Lyapunov orbit is a homoclinic trajectory of the planar Lyapunov orbit. Of course, the homoclinic trajectory that goes out from the orbit and the one that goes in do not generally coincide: they should intersect one each other with a very small angle. This phenomenon is known as splitting of separatrices. Finally, by sending those orbits to the RTBP coordinates, it is possible to see that the description provided by those plots is valid (and very accurate) up to a distance of L_1 a little bit bigger than 60% of the L_1-Earth distance.

3.2.3 The L_2 point of the Earth-Moon system

It is not difficult to repeat the computations of the last section for the L_2 point of the Earth-Moon system. The Hamiltonian restricted to the centre manifold is displayed in Table 2, and the estimates of the region of convergence are shown in Figure 5. Figure 6 contains the plots of the Poincaré sections, where the bifurcation that gives rise to the Halo orbits is also shown. As before, it is possible to check that this description is very accurate up to a half distance from L_2 to the Moon. As the results are very similar to the last case, we do not add further remarks.

3.2.4 The L_3 point of the Earth-Moon system

We have also performed these computations for the L_3 point. The main difference between this point and $L_{1,2}$ can be seen in Figure 1: while $L_{1,2}$ are strongly influenced by the two bodies, L_3 is influenced by the biggest primary but the effect of the smallest primary is almost neglectable. This implies that the dynamics near L_3 is rather close to the dynamics of a two body problem (that is very degenerate). This is the reason for the big coefficients shown in Table 3, that are responsible for the poor convergence radius shown in Figure 7: Hence, one must use very small values of the energy in order to be inside the region of convergence. This does not allow to go far enough to observe the bifurcation corresponding to the Halo orbits and, for this reason, we have not included the corresponding plots for this case.

So, the study of the behaviour around L_3 (including the computation of Halo orbits) is a difficult problem. Moreover, as far as we know, there are no astronautical or astronomical applications that require an accurate knowledge of the phase space around this point. We believe that, in case that this study were necessary, it would be better to look at it as a slightly perturbed two body problem rather than using the techniques discussed here.

k_1	k_2	k_3	k_4	h_k	k_1	k_2	k_3	k_4	h_k
2	0	0	0	9.3132294092164980e-01	0	0	2	2	1.6516656013507769e-01
0	2	0	0	9.3132294092164991e-01	4	1	0	0	3.0065634937222852e-01
0	0	2	0	8.9308808149867502e-01	2	3	0	0	-5.8388370855924443e-01
0	0	0	2	8.9308808149867525e-01	0	5	0	0	3.1707966658149511e-02
2	1	0	0	-8.3074621158508666e-01	2	1	2	0	2.4502956646982510e-01
0	3	0	0	6.5285116341699909e-02	0	3	2	0	-1.9424915041015245e-01
0	1	2	0	-6.4906335171207086e-01	0	1	4	0	8.2423593768551455e-03
4	0	0	0	-3.0986677967027330e-02	3	0	1	1	1.7854668840138077e-01
2	2	0	0	5.9388694902317307e-01	1	2	1	1	-4.2089157809945715e-01
0	4	0	0	-4.1582038336828324e-02	1	0	3	1	1.3900075305874218e-01
2	0	2	0	-4.7016550083469763e-02	2	1	0	2	-2.8565999503473249e-01
0	2	2	0	3.5694318621877408e-01	0	3	0	2	7.7193563104132376e-02
0	0	4	0	-1.7818840096908990e-02	0	1	2	2	-2.8562245235708378e-01
1	1	1	1	1.1056617867458479e-01	1	0	1	3	-7.5028466176853367e-02
2	0	0	2	2.1139923206390523e-01	0	1	0	4	4.3954249987303046e-02
0	2	0	2	-4.9839132339243322e-02					

Table 2: Coefficients, up to degree 5, of the Hamiltonian restricted to the centre manifold corresponding to the L_2 point of the Earth-Moon system. The exponents (k_1, k_2, k_3, k_4) refer to the variables (q_2, p_2, q_3, p_3), in this order.

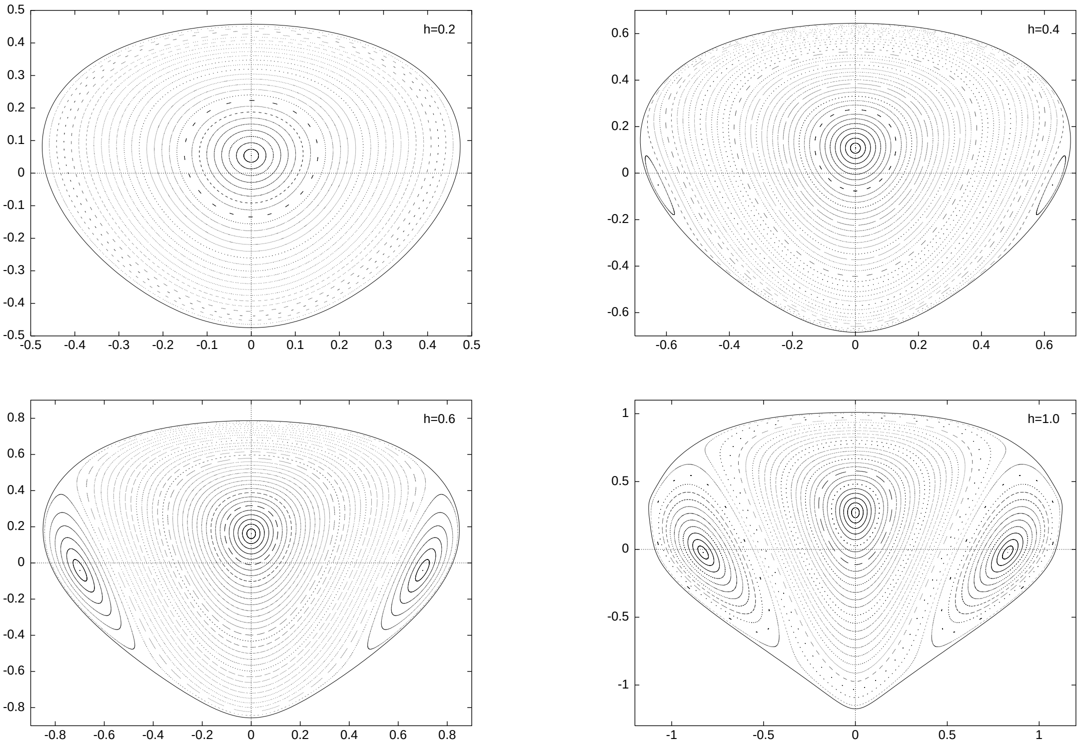

Figure 6: Poincaré sections of the centre manifold of L_2, corresponding to $h = 0.2$, 0.4 0.6 and 1.0.

k_1	k_2	k_3	k_4	h_k	k_1	k_2	k_3	k_4	h_k
2	0	0	0	5.0520994612145753e-01	0	0	2	2	7.1591406119636058e-01
0	2	0	0	5.0520994612145753e-01	4	1	0	0	2.1323011406157320e+03
0	0	2	0	5.0266571276387528e-01	2	3	0	0	-5.6249141438829110e+02
0	0	0	2	5.0266571276387528e-01	0	5	0	0	1.3204637130128873e+01
2	1	0	0	-5.6115912436382951e+00	2	1	2	0	5.2838311677563991e+02
0	3	0	0	9.3496383336128464e-01	0	3	2	0	-3.0623587048451135e+01
0	1	2	0	-1.4686056924068396e+00	0	1	4	0	1.5515423765627251e+01
4	0	0	0	7.6528931476095536e+00	3	0	1	1	1.8825389781246327e+00
2	2	0	0	1.3546730001510483e+01	1	2	1	1	-3.6872790343761423e+01
0	4	0	0	3.8069286794284551e-01	1	0	3	1	1.7599729630272192e+00
2	0	2	0	3.3499313360906959e+00	2	1	0	2	5.0848622203654816e+02
0	2	2	0	7.9659730977543119e-01	0	3	0	2	-2.9960960321274250e+01
0	0	4	0	3.5254807289843670e-01	0	1	2	2	2.7128291101879991e+01
1	1	1	1	4.0669264872473150e+00	1	0	1	3	-5.2867739300861096e+00
2	0	0	2	2.7355314621061146e+00	0	1	0	4	1.7913955620592070e+01
0	2	0	2	-1.3673249909233478e+00					

Table 3: Coefficients, up to degree 5, of the Hamiltonian restricted to the centre manifold corresponding to the L_3 point of the Earth-Moon system. The exponents (k_1, k_2, k_3, k_4) refer to the variables (q_2, p_2, q_3, p_3), in this order.

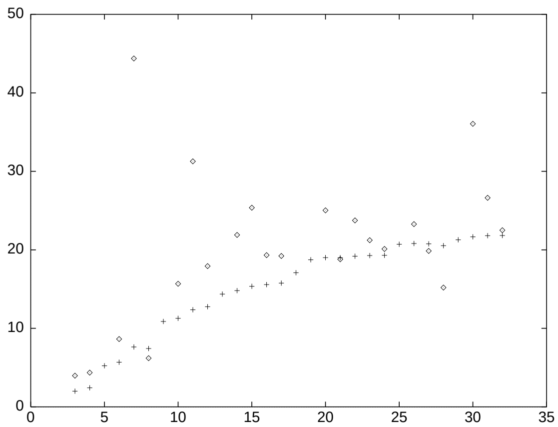

Figure 7: Horizontal axis: values of n. Vertical axis: the corresponding values of $r_n^{(1)}$ ($\diamond$) and $r_n^{(2)}$ ($+$) according to (21), for the L_3 case.

4 Semianalytical computation of invariant tori. The Lindstedt-Poincaré method

Here we focus on the computation of periodic and quasiperiodic solutions contained in the centre manifold. As we want to avoid using changes of variables, we will work directly on equations (14).

4.1 Lissajous Orbits

We follow the idea of the Lindstedt-Poincaré method to look for these 2-D invariant tori as a series expansion in two frequencies, which formally satisfies the equations of motion up to a selected order (to be defined later). The procedure, as we will see, is a recursion that determines the coefficients of each order from the ones corresponding to lower orders that have been computed in previous steps.

As a starting point we need the (non trivial) librating solutions of the linear part of (14),

$$\begin{aligned} \ddot{x} - 2\dot{y} - (1+2c_2)x &= 0, \\ \ddot{y} + 2\dot{x} + (c_2-1)y &= 0, \\ \ddot{z} + c_2 z &= 0, \end{aligned} \tag{22}$$

that can be written as

$$\begin{aligned} x(t) &= \alpha\cos(\omega_0 t + \phi_1), \\ y(t) &= \kappa\alpha\cos(\omega_0 t + \phi_1), \\ z(t) &= \beta\cos(\nu_0 t + \phi_2), \end{aligned}$$

where $\omega_0 = \sqrt{\frac{2-c_2+\sqrt{9c_2^2-8c_2}}{2}}$, $\nu_0 = \sqrt{c_2}$ and $\kappa = \frac{-(\omega_0^2+1+2c_2)}{2\omega_0}$ (see Section 2.1). The free parameters α and β, usually called in plane and out of plane amplitudes respectively, and ϕ_1, ϕ_2, from now on called the phases, give all the librating solutions of the linear part of the equations.

We note that, due to the autonomous character of the equations, only one phase is needed. Hence, a solution is determined by three parameters, α, β and a phase. Nevertheless we will keep two phases because, as we will see, the computations in both cases are exactly the same.

When we consider the nonlinear terms of the equations, we look for formal expansions in powers of the amplitudes α and β, of the type

$$\begin{aligned} x(t) &= \sum_{i,j=1}^{\infty}\left(\sum_{|k|\le i,\,|m|\le j} x_{ijkm}\cos(k\theta_1+m\theta_2)\right)\alpha^i\beta^j, \\ y(t) &= \sum_{i,j=1}^{\infty}\left(\sum_{|k|\le i,\,|m|\le j} y_{ijkm}\sin(k\theta_1+m\theta_2)\right)\alpha^i\beta^j, \end{aligned}$$

$$z(t) = \sum_{i,j=1}^{\infty} \left(\sum_{|k|\leq i,\, |m|\leq j} z_{ijkm} \cos(k\theta_1 + m\theta_2) \right) \alpha^i \beta^j,$$

where $\theta_1 = \omega t + \phi_1$ and $\theta_2 = \nu t + \phi_2$. Due to the presence of nonlinear terms the frequencies ω and ν can be kept no longer constant and they must be expanded as well in powers of the amplitudes: $\omega = \sum_{i,j=0}^{\infty} \omega_{ij}\alpha^i\beta^j$ and $\nu = \sum_{i,j=0}^{\infty} \nu_{ij}\alpha^i\beta^j$.

The goal is to compute the coefficients x_{ijkm}, y_{ijkm}, z_{ijkm}, ω_{ij} and ν_{ij} recurrently up to a finite order $i + j = n_f$ with the following meaning. Identifying the first coefficients of the general solution with the ones obtained from the solution of the linear part, we see that the non zero values are $x_{1010} = 1$, $y_{1010} = \kappa$, $z_{0101} = 1$, $\omega_{00} = \omega_0$ and $\nu_{00} = \nu_0$. The insertion of the expression of the solution of the linear part in (14) produces a remainder which are series in α, β, beginning with terms of order $i + j = 2$. In what follows, it is said that the solution is computed up to order $i + j = n$ when, after inserting the obtained expression for the solution into the equations, the remainder consists of three series beginning with terms of order $i + j = n + 1$.

Before going into the details of the computations we note that $x(t)$ and $z(t)$ are both written as a cosinus series and $y(t)$ as a sinus one. This can be done due to the symmetries of the problem and to the selected expression for the solution of the linear part. It is not difficult to see that if j is odd the coefficients x_{ijkm} and y_{ijkm} are zero, and if j is even the coefficients z_{ijkm} are zero. As it is usual in the Lindstedt-Poincaré method, we only work with coefficients such that $|k| \leq i$ and $|m| \leq j$ and, moreover, k and m must have the same parity as i and j respectively. Due to the symmetries of sinus and cosinus, we can assume that $k \geq 0$ and, when $k = 0$, we can assume $m \geq 0$. Finally, in the expansions of the frequencies ω and ν only terms with both i and j even appear. All these properties have been taken into account to save computing time and storage.

At the first step of the procedure we start with the series $x(t)$, $y(t)$ and $z(t)$ determined up to order one and the series ω and ν up to order zero. At a certain step we will have the solution up to order $n - 1$, this is, $x(t)$, $y(t)$ and $z(t)$ determined up to order $n - 1$ and ω and ν up to order $n - 2$ if $n - 1$ is odd, or up to order $n - 3$ if $n - 1$ is even. In any case, we will say that ω and ν are determined up to order $n - 2$, remembering that for odd orders the corresponding terms are zero.

Assume that we have computed the solution up to order $n - 1$. When we insert this expression in the right-hand side of the equations (14), we obtain three series determined up to order n. Denote by p, q and r these series, that are respectively of the same type as x, y and z. We are interested in findind the terms of order n of the solution by equating the (known) order n terms of p, q and r with the corresponding (and unknown) terms coming from the left hand side of equations (14). From now on (unless otherwise stated), and to simplify the notation, v_{ijkm} will refer to the terms with $i + j = n$ of a series v. When k and m are omitted it will refer to a frequency type series.

Hence, the order n of the equations must be equated from both sides of (14). In the left-hand side there appear some derivatives which can be computed in the following way,

$$\dot{x} = \frac{\partial x}{\partial \theta_1}\frac{d\theta_1}{dt} + \frac{\partial x}{\partial \theta_2}\frac{d\theta_2}{dt} = \omega\frac{\partial x}{\partial \theta_1} + \nu\frac{\partial x}{\partial \theta_2},$$

$$\ddot{x} \;=\; \omega^2\frac{\partial^2 x}{\partial\theta_1^2} + 2\omega\nu\frac{\partial^2 x}{\partial\theta_1\partial\theta_2} + \nu^2\frac{\partial^2 x}{\partial\theta_2^2}.$$

Similar expressions can be derived for $\dot{y}$, $\ddot{y}$ and $\ddot{z}$.

Each summand of the former expressions contains products of series of different type, for instance $\omega\frac{\partial x}{\partial\theta_1}$ in the first order derivatives and $\omega^2\frac{\partial^2 x}{\partial\theta_1^2}$ in the second order ones. Since the series x, y and z are known up to order $n-1$ and ω and ν up to order $n-2$, the order n of these products of series contains a known part which can be added to p_{ijkm}, q_{ijkm}, r_{ijkm} and an unknown part that consists of products of terms which have to be determined. Let us see this with more detail.

Let fv be one of the terms that appear in the computations of the first derivative (f denotes the series of a frequency and v denotes the derivative of a coordinate series). The known part of order n of fv is obtained multiplying the terms of order i_f of f with the terms of order j_v of v such that $i_f+j_v=n$, being $i_f=1,\dots,n-2$. The unknown part of order n appears when multiplying the respective parts of order 0 and n, and order $n-1$ and 1 of f and v. The following table summarizes the unknown parts of order n in the computations of the first derivatives of x and y. The symbol δ stands for Kronecker's delta.

f	v	$\omega\frac{\partial x}{\partial\theta_1}$	$\nu\frac{\partial x}{\partial\theta_2}$	$\omega\frac{\partial y}{\partial\theta_1}$	$\nu\frac{\partial y}{\partial\theta_2}$
0	n	$-\omega_{00}kx_{ijkm}$	$-\nu_{00}mx_{ijkm}$	$\omega_{00}ky_{ijkm}$	$\nu_{00}my_{ijkm}$
$n-1$	1	$-\omega_{i-1j}\delta_{1k}\delta_{0m}$	0	$\kappa\omega_{i-1j}\delta_{1k}\delta_{0m}$	0

If f is a frequency-type series and v a coordinate series (x, y or z), the following table sumarizes the unknown parts of order n in the computations of the second derivatives.

f	$\frac{\partial^2 v}{\partial\theta^2}$	$\omega^2\frac{\partial^2 v}{\partial\theta_1^2}$	$-2\omega\nu\frac{\partial^2 v}{\partial\theta_1\partial\theta_2}$	$\nu^2\frac{\partial^2 v}{\partial\theta_2^2}$
0	n	$-\omega_{00}^2k^2v_{ijkm}$	$-2\omega_{00}\nu_{00}kmv_{ijkm}$	$-\nu_{00}m^2v_{ijkm}$
$n-1$	1	$-f_{i-1j}v_{1010}\delta_{1k}\delta_{0m}$	0	$-f_{ij-1}v_{0101}\delta_{0k}\delta_{1m}$

The known parts of order n coming from the first and second derivatives of the left-hand side of equations (14) are added to p_{ijkm}, q_{ijkm} and r_{ijkm}. Let us denote by $\bar{p}_{ijkm}$, $\bar{q}_{ijkm}$ and $\bar{r}_{ijkm}$ the resulting values.

Let us give some details about the computation of the terms f_{i-1j} and f_{ij-1} of the former table. First, we note that both are terms of order $n-1$. They consist of an unknown part coming from the product of order zero of one serie against order $n-1$ of the another, plus a known part coming from the remaining products that produce order $n-1$. As in the previous table f_{i-1j} represents the terms of order $n-1$ of ω^2 and f_{ij-1} represents the terms of order $n-1$ of ν^2, we can write $f_{i-1j}=2\omega_{00}\omega_{i-1j}+\Omega_{i-1j}$ and $f_{ij-1}=2\nu_{00}\nu_{ij-1}+N_{ij-1}$, where Ω_{i-1j} and N_{ij-1} stand for the known parts of order $n-1$ we have just mentioned.

So, the linear system of equations for the unknown terms of order n can be written as,

$$\begin{aligned}
-\left(\varpi_{km}^2+1+2c_2\right)x_{ijkm}-2\varpi_{km}y_{ijkm}-2\left(\omega_{00}+\kappa\right)\omega_{i-1j}\delta_{1k}\delta_{0m} &= \bar{\bar{p}}_{ijkm},\\
-2\varpi_{km}x_{ijkm}+\left(c_2-1-\varpi_{km}^2\right)y_{ijkm}-2\left(\kappa\omega_{00}+1\right)\omega_{i-1j}\delta_{1k}\delta_{0m} &= \bar{\bar{q}}_{ijkm},\\
\left(c_2-\varpi_{km}^2\right)z_{ijkm}-2\nu_{00}\nu_{ij-1}\delta_{0k}\delta_{1m} &= \bar{\bar{r}}_{ijkm},
\end{aligned}\tag{23}$$

where $\varpi_{km} = k\omega_{00} + m\nu_{00}$, $\bar{\bar{p}}_{ijkm} = \bar{p}_{ijkm} + \Omega_{i-1j}\delta_{1k}\delta_{0m}$, $\bar{\bar{q}}_{ijkm} = \bar{q}_{ijkm} + \kappa\Omega_{i-1j}\delta_{1k}\delta_{0m}$ and $\bar{\bar{r}}_{ijkm} = \bar{r}_{ijkm} + N_{ij-1}\delta_{0k}\delta_{1m}$.

When $(k,m) \neq (1,0)$ and $(k,m) \neq (0,1)$ we can solve (23) to find x_{ijkm}, y_{ijkm} and z_{ijkm}. Note that, if the frequencies of the linearized system are nonresonant, the determinant of the matrix of this system is always different from zero, although it can be very small due to the small divisors problem. As usual, this problem becomes more relevant for high orders.

When $(k,m) = (1,0)$ (this can only happen when n is odd) the determinant of the x-y part in the first two equations of (23) is zero. So, we normalize taking $x_{ij10} = 0$ and we can solve for y_{ij10}, ω_{i-1j}. Finally z_{ij10} is determined solving $(c_2 - \omega_{00}^2)z_{ij10} = \bar{p}_{ij10}$.

When $(k,m) = (0,1)$ we can determine x_{ij01} and y_{ij01} by solving the first two equations of (23). As in the third equation the coefficient of z_{ij01} is zero, we normalize the solution taking $z_{ij01} = 0$ and solving $-2\nu_{00}\nu_{ij-1} = \bar{p}_{ij01} + N_{ij-1}$ for ν_{ij-1}.

4.2 Halo Orbits

Halo orbits are periodic orbits which bifurcate from the planar Lyapunov periodic orbits when the in plane (or intrinsic) and out of plane (or normal) frequencies are equal. This is a 1:1 resonance that appear as a consequence of the nonlinear terms of the equations and, hence, we have to look for these 1-D invariant tori as series expansion with a single frequency.

As Halo orbits are due to the nonlinear terms of the equations, they do not appear in the linearized equations (22). In order to apply the Lindstedt-Poincaré procedure we modify the equations of motion (14) by adding the product of the factors Δ and z to the third equation,

$$\begin{aligned} \ddot{x} - 2\dot{y} - (1+2c_2)x &= \sum_{n\geq 2} c_{n+1}(n+1)T_n, \\ \ddot{y} + 2\dot{x} + (c_2-1)y &= y\sum_{n\geq 2} c_{n+1}R_{n-1}, \\ \ddot{z} + c_2 z &= z\sum_{n\geq 2} c_{n+1}R_{n-1} + \Delta z. \end{aligned} \tag{24}$$

We will look for 1-D invariant tori of these equations, with the condition $\Delta = 0$. In the procedure, the factor Δ is expanded as a frequency-type series, this is, $\Delta = \sum_{i,j=0}^{\infty} d_{ij}\alpha^i\beta^j$. The coefficients d_{ij} will be computed recurrently.

We start looking for the (non trivial) librating solutions with one frequency of the linear part of (24),

$$\begin{aligned} \ddot{x} - 2\dot{y} - (1+2c_2)x &= 0, \\ \ddot{y} + 2\dot{x} + (c_2-1)y &= 0, \\ \ddot{z} + c_2 z &= d_{00}z. \end{aligned}$$

It is not difficult to see that they can be written as

$$x(t) = \alpha\cos(\omega_0 t + \phi),$$

$$\begin{aligned} y(t) &= \kappa\alpha\cos(\omega_0 t+\phi), \\ z(t) &= \beta\cos(\omega_0 t+\phi), \end{aligned}$$

with $d_{00} = c_2 - \omega_0^2$ and where $\omega_0 = \sqrt{\frac{2-c_2+\sqrt{9c_2^2-8c_2}}{2}}$, $\kappa = \frac{-(\omega_0^2+1+2c_2)}{2\omega_0}$ and ϕ is an arbitrary phase.

As in the case of Lissajous orbits, α and β are called the in plane and out of plane amplitudes respectively. Of course, Halo orbits depend only on one frequency or one amplitude since they are 1-D invariant tori. The relationship between α and β is contained in the condition $\Delta = 0$ which defines implicitely $\alpha = \alpha(\beta)$. We note that, at the current step, Halo orbits are determined up to order 1, and $\Delta = 0$ is read as $d_{00} = 0$, showing again that there are not Halo orbits in the linear part of the equations.

When we consider the nonlinear terms of (24), we look for formal expansions in powers of the amplitudes α and β of the type

$$\begin{aligned} x(t) &= \sum_{i,j=1}^{\infty}\left(\sum_{|k|\le i+j} x_{ijk}\cos(k\theta)\right)\alpha^i\beta^j, \\ y(t) &= \sum_{i,j=1}^{\infty}\left(\sum_{|k|\le i+j} y_{ijk}\sin(k\theta)\right)\alpha^i\beta^j, \\ z(t) &= \sum_{i,j=1}^{\infty}\left(\sum_{|k|\le i+j} z_{ijk}\cos(k\theta)\right)\alpha^i\beta^j, \end{aligned}$$

where $\theta = \omega t + \phi$ and, as in the case of 2-D invariant tori, the frequency ω must be expanded as $\omega = \sum_{i,j=0}^{\infty}\omega_{ij}\alpha^i\beta^j$. Moreover, now we have the expansion of the constraint $\Delta = \sum_{i,j=0}^{\infty} d_{ij}\alpha^i\beta^j = 0$.

As in the computation of Lissajous orbits, the symmetries of the problem allow to only consider terms with j even for the series $x(t)$, $y(t)$ and with j odd for the series $z(t)$. Moreover, we can restrict ourselves to the case in which $0 \le k \le i+j$, having k and $i+j$ the same parity. Finally, the frequency series ω and Δ only contain terms with both i and j even.

The final goal is to compute the coefficients x_{ijk}, y_{ijk}, z_{ijk}, ω_{ij} and d_{ij} recurrently up to a finite order $i+j = n_f$, starting with the (pseudo) solution of the linear part whose non zero values are $x_{101} = 1$, $y_{101} = \kappa$, $z_{011} = 1$, $\omega_{00} = \omega_0$ and $d_{00} = c_2 - \omega_0^2$.

As it is usual in this kind of Lindstedt-Poincaré procedure, at some step we will have the series $x(t)$, $y(t)$ and $z(t)$ determined up to order $n-1$ and the series ω and Δ up to order $n-2$ (we recall that when $n-1$ is even, the terms of order $n-2$ of these series are zero). When we insert these expansions in the right hand side of the equations (24) we obtain the series p_{ijk}, q_{ijk}, r_{ijk} and Δz (note that the term Δz is not included in r_{ijk}). Of course, p_{ijk}, q_{ijk} and r_{ijk} are of the same type as x, y and z respectively. Note that they are determined up to order $i+j = n$, and that the product Δz is determined up to order $n-2$ if $n-1$ is odd, or up to order $n-3$ if $n-1$ is even.

Next, we have to compute the part of order n of the derivatives with respect to time, $\dot{x}$, $\dot{y}$, $\ddot{x}$, $\ddot{y}$ and $\ddot{z}$. As in the previous section, these computations involve products of series of different type such as $\dot{x} = \omega \frac{\partial x}{\partial \theta}$ or $\ddot{x} = \omega^2 \frac{\partial^2 x}{\partial \theta^2}$. The same statement holds for the computation of the part of order n of Δz. As in the previous section, the part of order n of these products consists of an already known part and of an unknown one. The known part is added to the corresponding series p_{ijk}, q_{ijk} or r_{ijk} to obtain the new series $\bar{p}_{ijk}$, $\bar{q}_{ijk}$ and $\bar{r}_{ijk}$. The unknown terms are summarized in the following tables.

f	v	$\omega \frac{\partial x}{\partial \theta}$	$\omega \frac{\partial y}{\partial \theta}$	Δz
0	n	$-\omega_{00} k x_{ijk}$	$\omega_{00} k y_{ijk}$	$d_{00} z_{ijk}$
$n-1$	1	$-\omega_{i-1j}\delta_{1k}$	$\omega_{i-1j}\kappa\delta_{1k}$	$d_{ij-1}\delta_{1k}$

f	$\frac{\partial^2 v}{\partial \theta^2}$	$\omega^2 \frac{\partial^2 x}{\partial \theta^2}$	$\omega^2 \frac{\partial^2 y}{\partial \theta^2}$	$\omega^2 \frac{\partial^2 z}{\partial \theta^2}$
0	n	$-\omega_{00}^2 k^2 x_{ijk}$	$-\omega_{00}^2 k^2 y_{ijk}$	$-\omega_{00}^2 k^2 z_{ijk}$
$n-1$	1	$-f_{i-1j}\delta_{1k}$	$-f_{i-1j}\kappa\delta_{1k}$	$-f_{ij-1}\delta_{1k}$

In the second table, f denotes the series corresponding to ω^2. Note that its $n-1$ order terms, f_{i-1j} and f_{ij-1}, are made of known and unknown parts, $f_{i-1j} = 2\omega_{00}\omega_{i-1j} + \Omega_{i-1j}$ and $f_{ij-1} = 2\omega_{00}\omega_{ij-1} + \Omega_{ij-1}$, where Ω_{i-1j} and Ω_{ij-1} denotes the known ones.

Finally, we can write the linear system of equations for the unknown terms of order n,

$$\begin{aligned}
-\left(k^2\omega_{00}^2 + 1 + 2c_2\right) x_{ijk} - 2k\omega_{00} y_{ijk} - 2\left(\omega_{00} + \kappa\right)\omega_{i-1j}\delta_{1k} &= \bar{p}_{ijk} + \Omega_{i-1j}\delta_{1k}, \\
-2k\omega_{00} x_{ijk} + \left(c_2 - 1 - k^2\omega_{00}^2\right) y_{ijk} - 2\left(\kappa\omega_{00} + 1\right)\omega_{i-1j}\delta_{1k} &= \bar{q}_{ijk} + \kappa\Omega_{i-1j}\delta_{1k}, \\
\left(c_2 - k^2\omega_{00}^2 - d_{00}\right) z_{ijk} - d_{ij-1}\delta_{1k} &= \bar{r}_{ijk} + \Omega_{ij-1}\delta_{1k} + 2\omega_{00}\omega_{ij-1}\delta_{1k}.
\end{aligned} \tag{25}$$

When $k \neq 1$ we can solve (25) for x_{ijk}, y_{ijk} and z_{ijk}. When $k = 1$ the determinant of the xy part and the coefficient of z_{ijk} are zero. Then we can normalize by taking $x_{ij1} = 0$, $z_{ij1} = 0$, and solving the first two equations of (25) to find y_{ij1} and ω_{i-1j}. Finally the third equation is solved to obtain d_{ij-1}.

4.3 Numerical results

The algorithms presented for the semianalytical computation of the Lissajous and Halo orbits have been implemented using Fortran 77 language. As in the computation of the centre manifold, commercial algebraic manipulators are much less efficient dealing with expansions, specially in the case where symmetries can be efficiently implemented in the computations. The use of an ad hoc code allows us to reach very high orders (obtaining then very accurate solutions) in a short time. Table 4 summarizes the amount of RAM memory and CPU time used in some of these computations. In Tables 5 and 6 show the coefficients of the Halo and Lissajous expansions around L_1 in the Earth-Sun system, up to order 3. Typical plots of Halo orbits, vertical periodic (Lyapunov) orbits and Lissajous trajectories are presented in Figures 8, 9 and 10, respectively.

The accuracy of the expansions has been tested against numerical integration. For this pourpose, some initial conditions have been computed by tabulating the series expansions up to different orders. Then, these initial conditions have been integrated (numerically) during π units of adimensional time. The final coordinates obtained from this numerical

N	Halo		Lissajous	
15	113.2 Kb	<1s.	350.8 Kb	<1s.
17	171.7 Kb	<1s.	577.9 Kb	1s.
19	250.3 Kb	<1s.	909.3 Kb	3s.
21	353.2 Kb	1s.	1377.2 Kb	6s.
23	484.8 Kb	2s.	2019.9 Kb	12s.
25	650.1 Kb	3s.	2882.1 Kb	22s.
27	854.2 Kb	6s.	4015.8 Kb	38s.
29	1103.0 Kb	9s.	5480.2 Kb	65s.
31	1402.4 Kb	14s.	7342.9 Kb	107s.
33	1758.9 Kb	21s.	9679.8 Kb	173s.
35	2179.2 Kb	30s.	12576.0 Kb	269s.
37	2670.6 Kb	43s.	16126.3 Kb	420s.
39	3240.7 Kb	59s.	20435.4 Kb	641s.
41	3897.4 Kb	82s.	25618.8 Kb	940s.
43	4649.1 Kb	111s.	31803.1 Kb	1389s.
45	5504.5 Kb	148s.	39126.5 Kb	2003s.

Table 4: Computer time (in seconds, for an HP 712/100) and memory (in Kilobytes) for several degrees (N) of the Lindstedt-Poincaré computations.

i	j		ω_{ij}	d_{ij}
0	0		.2086453564223108E+01	-.2922144594039562E+00
2	0		-.1720616528118310E+01	.1596560311526045E+02
0	2		.2526665927441598E+00	-.1740900798763014E+01
i	j	k	x_{ijk} or z_{ijk}	y_{ijk}
1	0	1	.1000000000000000E+01	-.3229268251936296E+01
0	1	1	.1000000000000000E+01	
2	0	0	.2092695724506777E+01	-.4778922922033039E+01
2	0	2	-.9059648301914131E+00	-.4924458783826867E+00
0	2	0	.2482976576916406E+00	.0000000000000000E+00
0	2	2	.1044641085314726E+00	-.6074645997077919E-01
1	1	0	-.1040596322643552E+01	
1	1	2	.3468654408811841E+00	
3	0	1	.0000000000000000E+00	.2845081624743493E+01
3	0	3	-.7938202440824402E+00	-.8857008912091187E+00
1	2	1	.0000000000000000E+00	.4316928130485082E+00
1	2	3	.8268538161313826E-01	.2301983693229456E-01
2	1	3	.3980954407770784E+00	
0	3	3	-.1904387085744166E-01	

Table 5: Coefficients, up to order 3, of the Lindstedt-Poincaré expansion of the Halo orbits about L_1 in the Earth-Sun system (in this case, μ=3.040423398444176E-06 and γ=0.1001097722778141E-01).

i	j			ω_{ij}	ν_{ij}
0	0			.2086453564223108E+01	.2015210662996640E+01
2	0			-.1720616528118309E+01	.2227430750989766E+00
0	2			.2581841437578153E-01	-.1631915758176957E+00
i	j	k	m	x_{ijk} or z_{ijk}	y_{ijk}
1	0	1	0	.1000000000000000E+01	-.3229268251936296E+01
0	1	0	1	.1000000000000000E+01	
2	0	0	0	.2092695724506778E+01	-.4778922922033039E+01
2	0	2	0	-.9059648301914133E+00	-.4924458783826869E+00
0	2	0	0	.2482976576916407E+00	.0000000000000000E+00
0	2	0	2	.1108251822042930E+00	-.6776373426177420E-01
1	1	1	-1	-.1116868267568415E+01	
1	1	1	1	.3549452858304732E+00	
3	0	1	0	.0000000000000000E+00	.2845081624743493E+01
3	0	3	0	-.7938202440824405E+00	-.8857008912091185E+00
1	2	1	-2	-.1499994891576764E+01	-.4841968041750657E+01
1	2	1	0	.0000000000000000E+00	.2875532315811784E+00
1	2	1	2	.8387777659811270E-01	.2082881844639578E-01
2	1	2	-1	.1216565813734685E+02	
2	1	2	1	.4060793036977860E+00	
0	3	0	3	-.1952722175104363E-01	

Table 6: Coefficients, up to order 3, of the Lindstedt-Poincaré expansion of the Lissajous orbits about L_1 in the Earth-Sun system.

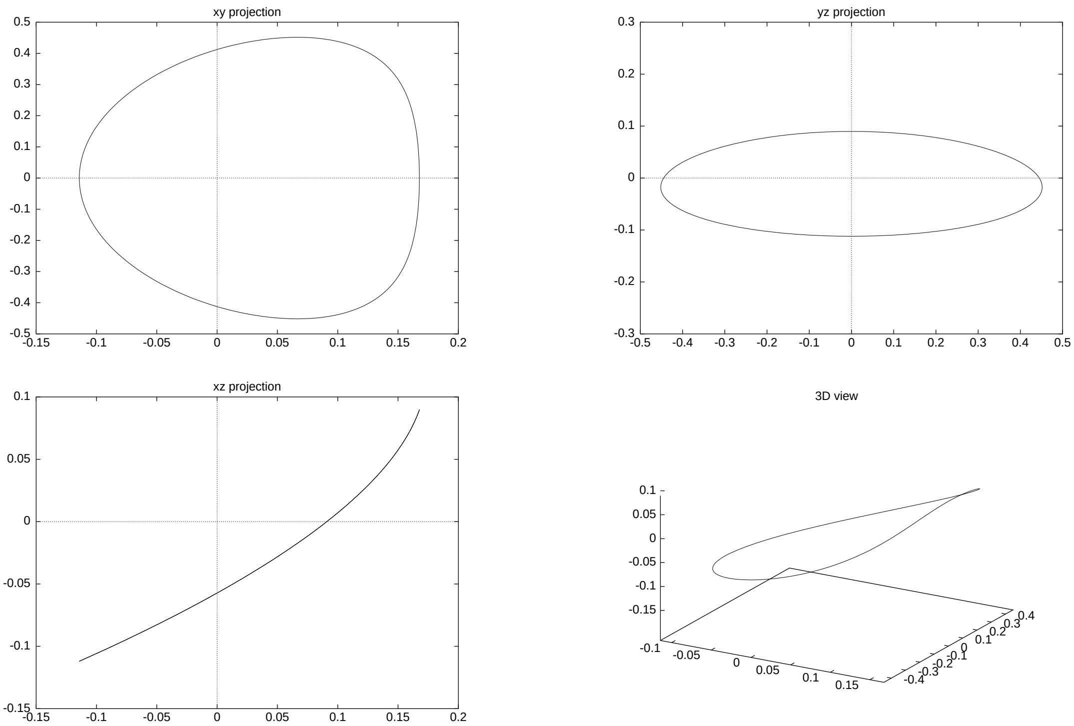

Figure 8: Projections on the coordinate planes and a 3D representation of a Halo orbit about L_1 in the Earth-Sun System with $\beta = 0.1$

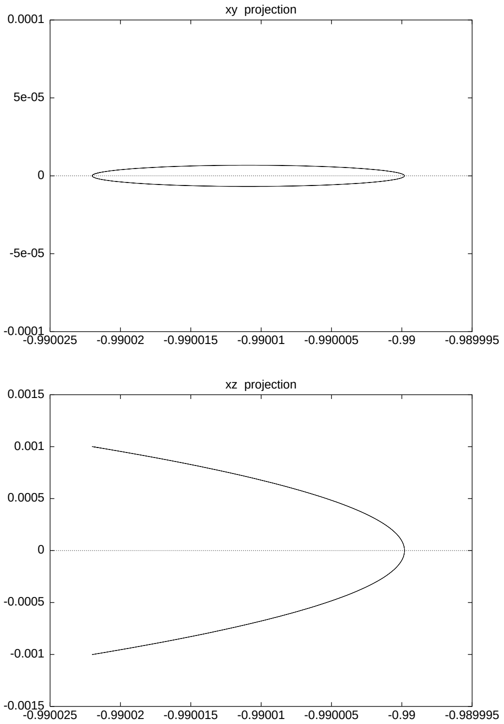

Figure 9: Projections on the coordinate planes and a 3D representation of a vertical periodic orbit about L_1 in the Earth-Sun System and with $\alpha = 0.0$ and $\beta = 0.1$

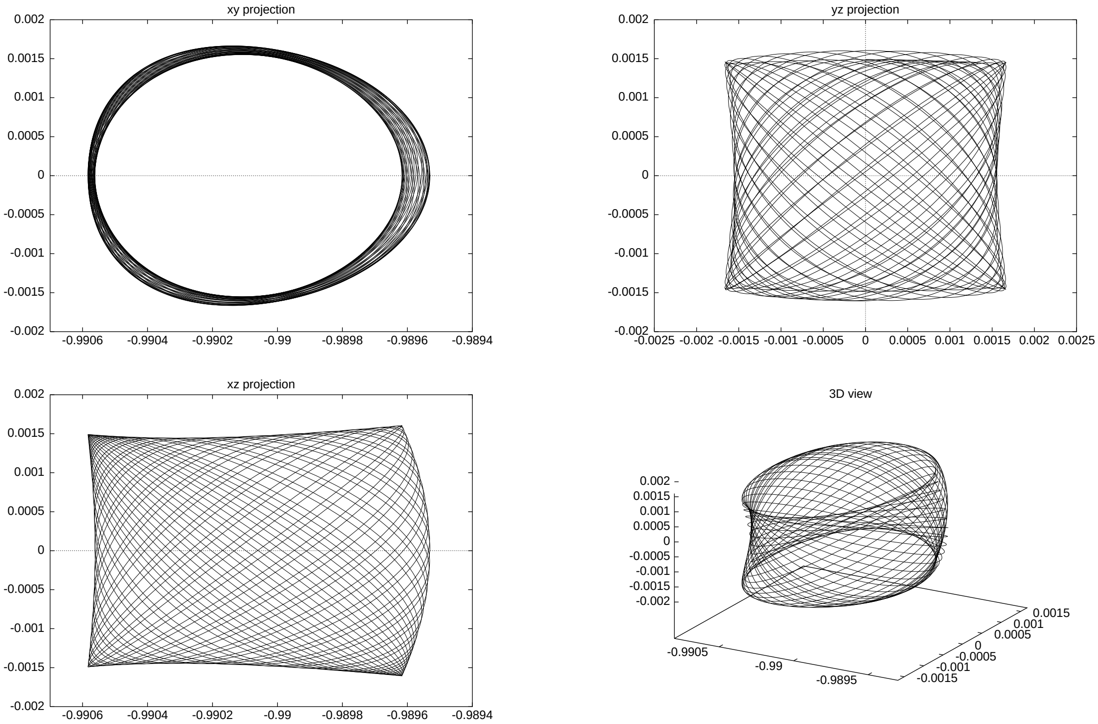

Figure 10: Projections on the coordinate planes and a 3D representation of a Lissajous orbit about L_1 in the Earth-Sun System and with $\alpha = 0.05$ and $\beta = 0.15$

integration have been compared with the coordinates given by the series expansion at time π. If the difference is lower than 10^{-6} adimensional RTBP units we say that the initial condition is accurate (in the sense that it "almost" correspond to a periodic or quasiperiodic trajectory). This test has been implemented only using the three spatial coordinates. Similar results are obtained using positions and velocities. The threshold has been selected to be 10^{-6} because, due to the unstability of the orbits around the collinear points, an error of this amount in position coordinates after π units of time, implies an error of about 100 meters in the initial conditions for the Earth-Sun system. This is because errors increase by a factor close to 1500 after π units of time. Other thresholds could have been selected, but the qualitative results are very similar to the ones presented.

The convergence regions for the case of Lissajous orbits are represented in Figure 11, using as example the expansion around L_1 for the Earth-Sun system. Each continuous line represents the boundary of the convergence region (according to the above mentioned criterion) for a selected order of truncation of the expansion. Given any couple (α, β) inside the region of convergence, the error after the numerical integration is less than the selected threshold for all the fases corresponding to the different initial conditions. A similar plot is used and discussed in [6].

The same test has been done for the case of Halo orbits. In this case the expansion only depends on one amplitude. The maximum β amplitude reached for some orders is given in Table 7.

order	β ampl.
11	0.196
15	0.336
21	0.461
25	0.502
31	0.557
35	0.604

Table 7: Maximum β amplitude which gives the region of convergence using the criterion explained in the text, for the case of Halo orbits around L_1 in the Earth-Sun system.

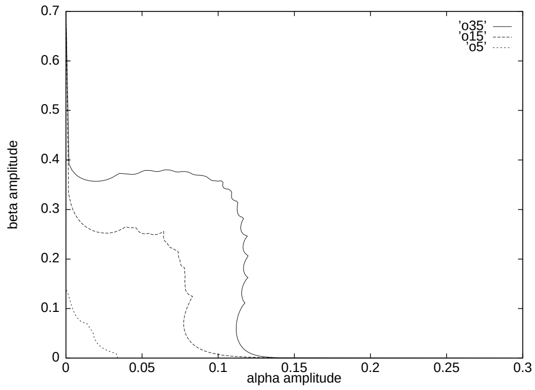

Figure 11: Convergence regions of the Lindstedt-Poincaré expansion of the Lissajous orbits around L_1 in the Earth-Sun system according to the criterion explained in the text. The different lines correspond to orders 5, 15 and 35.

Acknowledgements

The authors want to thank Carles Simó for interesting discussions and remarks. This research has been supported by the Spanish grant DGICYT PB94–0215, the EC grant ERBCHRXCT940460 and the Catalan grant CIRIT 1996SGR–00105. Part of this work was done while À. J. was visiting TICAM (Univ. of Texas).

References

[1] Cobos J., Simó C.: *Reduction to the Central Manifold around a Collinear Libration Point of the Restricted Three Body Problem*, to appear in the Proceedings of the XV CEDYA / V CMA held in Vigo (1997).

[2] Eliasson L. H.: *Perturbations of Stable Invariant Tori for Hamiltonian Systems*, Ann. Sc. Norm. Super. Pisa, Cl. Sci., Ser. IV, 15:1 (1988), pp. 115–147.

[3] Farquhar R. W.: *Halo-Orbit and Lunar-Swingby Missions of the 1990's*, Acta Astronautica 24 (1991), pp. 227–234.

[4] Farquhar R. W., Muhonen D. P., Newman C., Heuberger H.: *The first libration point satellite. Mission overview and flight history*, AAS/AIAA Astrodynamics Spec. Conf. (1979).

[5] Giorgilli A., Delshams A., Fontich E., Galgani L., Simó C.: *Effective Stability for a Hamiltonian System Near an Elliptic Equilibrium Point, with an Application to the Restricted Three Body Problem*, J. Diff. Eq. 77 (1989), pp. 167–198.

[6] Gómez G., Jorba A., Masdemont J., Simó C.: Study Refinement of Semi-Analytical Halo Orbit Theory, ESOC Contract 8625/89/D/MD(SC), Final Report (1991).

[7] Gómez G., Llibre J., Martínez R., Simó C.: Station Keeping of Libration Point Orbits, ESOC Contract 5684/83/D/JS(SC), Final Report (1985).

[8] Gómez G., Masdemont J., Simó C.: *Lissajous Orbits around Halo Orbits*, Advances in the Astronautical Sciences 95 (1997), pp. 117–134.

[9] Gómez G., Masdemont J., Simó C.: *Quasihalo Orbits associated with Libration Points*, preprint (1998).

[10] Howell K. C., Barden B. T., Wilson R. S., Lo M. W.: *Trajectory Design Using a Dynamical Systems Approach with Application to Genesis*, AAS Paper 97-709. AAS/AIAA Astrodynamics Specialist Conference, Sun Valley, Idaho (1997).

[11] Howell K. C., Pernicka H. J.: *Numerical Determination of Lissajous Trajectories in the Restricted Three-Body Problem*, Celestial Mechanics 41 (1988), pp. 107–124.

[12] Huber M. C. E. et al.: *The History of the SOHO Mission*, ESA Bulletin 86 (1996), pp. 25–35.

[13] Jorba À.: *A Methodology for the Numerical Computation of Normal Forms, Centre Manifolds and First Integrals of Hamiltonian Systems*, preprint (1998). To get a copy, look at `http://www.maia.ub.es/dsg/preprints`.

[14] Jorba À., Llave R.: *Regularity properties of center manifolds and applications*, in progress.

[15] Jorba À., Masdemont J.: *Nonlinear Dynamics in an Extended Neigbourhood of the Translunar Libration Point*, Hamiltonian Systems with Three or More Degrees of Freedom, C. Simó (Ed.), NATO Adv. Sci. Inst. Ser. C Math. Phys. Sci. Kluwer, Dordrecht, Holland (to appear).

[16] Jorba À., Villanueva J.: *On the Normal Behaviour of Partially Elliptic Lower Dimensional Tori of Hamiltonian Systems*, Nonlinearity 10 (1997), pp. 783–822.

[17] Jorba À., Villanueva J.: *On the Persistence of Lower Dimensional Invariant Tori under Quasi-Periodic Perturbations*, Journal of Nonlinear Science 7 (1997), pp. 427–473.

[18] Jorba À., Villanueva J.: *Numerical Computation of Normal Forms around some Periodic Orbits of the Restricted Three Body Problem*, Physica D 114 (1998), pp. 197–229.

[19] Poincaré H.: Les Méthodes Nouvelles de la Mécanique Céleste, Gauthier-Villars (1892, 1893, 1899).

[20] Simó C.: *Effective computations in celestial mechanics and astrodynamics*, lectures given at CISM Course on Modern Methods of Analytical Mechanics and their Applications, Udine, Italy (1997).

[21] Richardson D. L.: *A Note on a Lagrangian Formulation for Motion about the Collinear Points*, Celestial Mechanics 22 (1980), pp. 231–236.

[22] Richardson D. L.: *Halo orbit formulation for the ISEE-3 mission*, J. Guidance and Control 3 (1980), pp. 543–548.

[23] Szebehely V.: Theory of Orbits, Academic Press (1967).